

---

## NUMERICAL SIMULATIONS WITH THE USAGE OF HIGH ORDER ACCURACY METHODS

**Aleš Jirk, Josef Brechler**

**Charles University, Faculty of Mathematics and Physics, Department of Meteorology and Environment Protection, Prague**

### Abstract

In this contribution result of the test computations are presented. The configuration of these tests problems were as follow: 3D lid-driven cavity flows for different Reynolds numbers, Taylor-Green vortex and flows past an obstacle under various Reynolds numbers. The used model of the incompressible and low Mach number flow consists of the Navier–Stokes equations and the incompressible form of the continuity equation. To solve the system of equations the conservative high order methods were used. Convective terms of the N.-S. equations were computed using the 5<sup>th</sup> order weighted essentially non oscillatory (WENO) scheme. Turbulence (in case of the high Reynolds numbers) was modelled using the implicit large eddy simulation (ILES) method. Time integration is based on the application of the explicit TVD Runge-Kutta scheme.

### Introduction

Any atmospheric flow within the atmospheric boundary layer is turbulent. In this contribution, we focus on the problem of laminar and turbulent flow in 3D.

High-order accuracy is required in the simulation of turbulence in order to capture both the large- and small-scale structures of the flow. To prevent the occurrence of undesired spurious oscillations in our numerical modelling, we employed the finite volume approach with higher-order (fifth-order) WENO reconstruction. The turbulent model ILES goes hand in hand with WENO schemes. It is a form of Large Eddy Simulations (LES) in which the large energy containing structures are resolved, whereas the smaller, more isotropic, structures are filtered out and, therefore, their effects need to be modeled. For temporal discretization, we employed the explicit TVD (Total-Variation diminishing) Runge–Kutta (R–K) scheme. For splitting computational domain the finite volume method is used.

To test the applicability of this approach, we choose a problem involving flow in a cavity, around a cube in a channel. And a fundamental case The Taylor-Green Vortex (TGV) that has been traditionally used as prototype for vortex stretching and the consequent production of small-scale eddies, to investigate the basic dynamics of transition to turbulence (Drikakis et al.) and (Don et al. 2002). The lid-driven cavity flow case and the flow past an obstacle are computed for several values of Reynolds number. And the TGV problem is solved for different grids, Courant–Friedrichs–Lewy (CFL) computational stability conditions and Reynolds numbers.

### Governing system

To describe a fluid motion the equations representing the conservation laws of various quantities are used. They are the Navier-Stokes equations (1) for momentum conservation and these three equations are completed with the continuity relation (2) in incompressible form for the conservation of mass. All these equations (1-2) are evolved in Jirk 2008 and they are written in a non-dimensional form.

$$\frac{\partial v_i}{\partial t} + \frac{\partial v_i v_k}{\partial x_k} = -\frac{\partial p}{\partial x_i} + \frac{1}{\text{Re}} \Delta v_i \quad (1)$$

$$\frac{\partial v_i}{\partial x_i} = 0 \quad (2)$$

### Numerical method

For the spatial discretization of the governing equations (1-2) the finite volume method is used (see, for example, Ferziger, Perić 1997 or McDonough 2003). The advection terms in (1) are reconstructed by WENO scheme (Liu et al. 1994) that was extended from ENO scheme (Harten et al. 1987). A key idea in WENO scheme is a linear combination of lower order fluxes or reconstruction to obtain a higher order approximation. Both ENO and WENO schemes use the idea of adaptive stencils to automatically achieve high order accuracy and non-oscillatory property near discontinuities. In this work the WENO scheme of the fifth order accuracy has been used. For the computation of the temporal partial derivation in (1) there has been used the explicit TVD Runge-Kutta scheme of the third order accuracy (Gottlieb, Shu 1998). This scheme has CFL=1. For computing of viscous terms in (1) there is used Crank-Nicholson method (Kim et al. 2001). The fractional-step method (Brown et al. 2001) has been employed for solution of the Navier-Stokes equations (1) and continuity relation (2). This approach un-groups the solution of equations into several steps. In this work the three step method has been applied. For the simulation of the obstacle the second order accuracy immersed boundary method (Kim et al. 2001) is implemented. The turbulent model ILES (used in the work) does not require an explicitly computed sub-grid scale (SGS) model and it is implemented due to usually non-linear, regularization mechanism as e.g. WENO (Grinstein et al. 2007).

### Results, discussion

In this contribution the three cases of 3D non-linear flow have been simulated. The first one is a lid-driven cavity flow, the second case deals with the flow past an obstacle and the third one is Taylor-Green vortex problem.

#### 3D Lid-driven cavity flow

It is computed the flow motion in the cube. The sketch describing the cross-section xz geometry of the solved problem is displayed in Figure 1 together with the boundary conditions used.

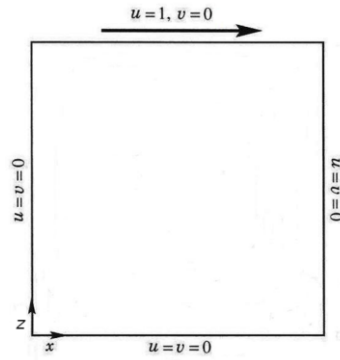


**Figure 1.** Configuration used in lid-driven cavity problem and coordinate system, cross-section x-z

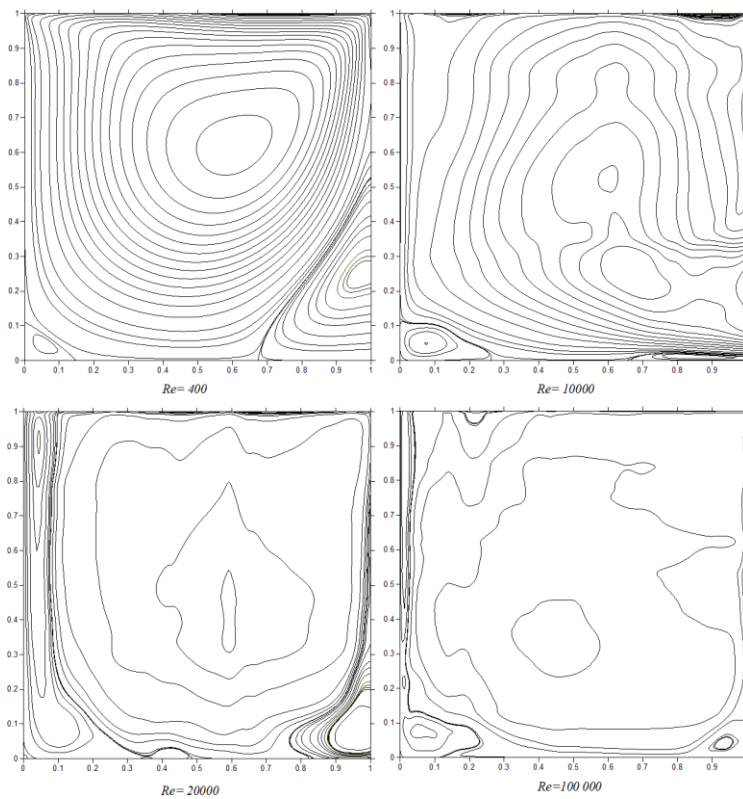


**Figure 2.** Lid-driven cavity case, cross-section xz, streamlines

The boundary conditions are stated as the Dirichlet boundary condition for the components of velocity.  $v=w=0$  on all boundaries,  $u=0$  in the side and bottom boundaries,  $u=1$  on the top boundary. CFL condition is chosen 0.3. The computations were carried out for the several values of Reynolds numbers, from the lowest 400 to 100 000.

In the Figure 2 there are depicted cross-section xz of flow field in dimensionless time  $t=36$  for  $160^3$  computational cells described with streamlines. In the Figure 3 there are shown y-component of vorticity for the same results as in Figure 2. As it can be seen with the increase of value of Reynolds number, the primer vortex is decaying. And a lot of secondary vortexes are pronounced.

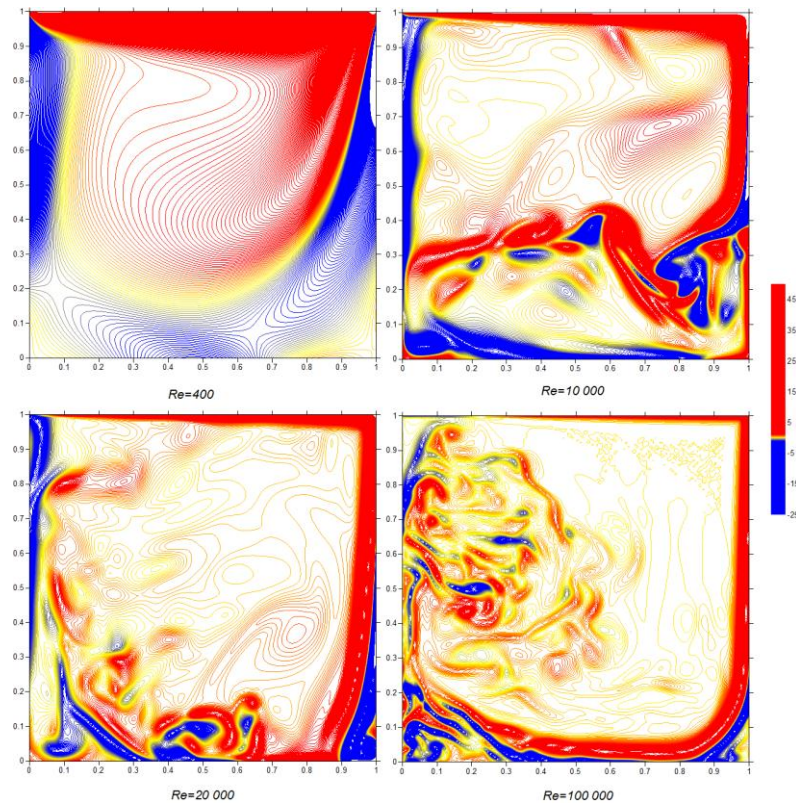


**Figure 3.** Lid-driven cavity case, cross-section xz, y-component of vorticity

For Reynolds number equal to 20 000 the vectors of velocity in 3D view and xz cross-section are depicted in the figure 4.

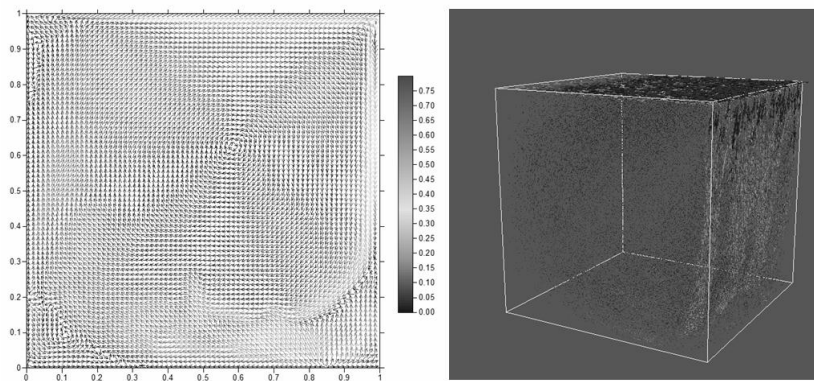


**Figure 4.** Lid-driven cavity case, cross-section xz velocity vectors (left) and 3D velocity view (right),  $Re = 20\,000$

### Flow past an obstacle

In this case it is modelled 3D flow past a cube, which is located in the middle of computed area (area has these proportions in dimensionless form: length  $L=40$  and width and height  $H=12$ ) in distance 12 from the inflow. As entry conditions there is used Dirichlet condition  $v=w=0, u=1$ . At the exit of flow are stated Neumann conditions  $\frac{\partial u}{\partial x} = \frac{\partial v}{\partial x} = 0$ . In the sides of computed area there are used periodic boundary conditions. The spatial step is 0.125. The CFL condition is chosen 0.3. Reynolds numbers are chosen 200, 5000 and 20 000.

In the Figure 5 there is depicted stable flow for Re 200. With the compare of 2D of the same case stable flow is pronounced for Re 30 and smaller. It was also computed for higher Reynolds number 5000 and 20 000 and the results are shown in the Figure 6. In contrast with case of low Reynolds number the vortex street behind obstacle is pronounced. All figures are shown in non-dimensional time  $t=50$ .

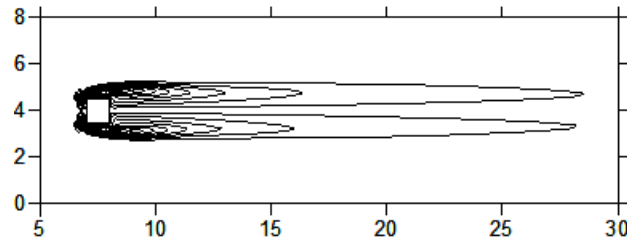


**Figure 5.** Flow past an obstacle, cross-section xz, y-component of vorticity for Re 200

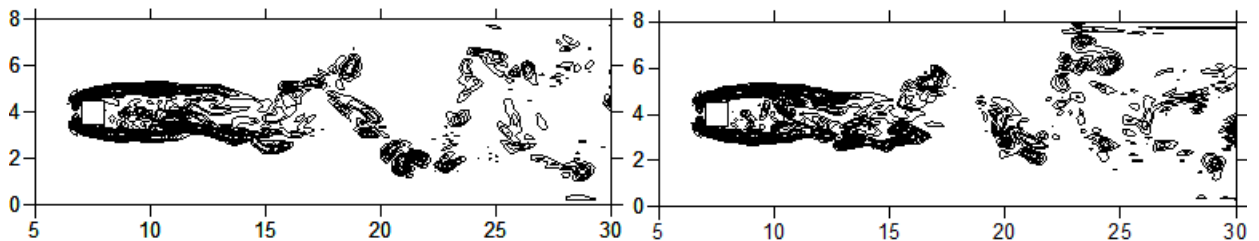


**Figure 6.** Flow past an obstacle, cross-section xz, y-component of vorticity: Re 5000 (left) and Re 20 000 (right)

### Taylor-Green vortex case

Configuration of this case here involves triple-periodic boundary conditions enforced on a cubical domain with box side length  $2\pi$  using  $160^3$  evenly spaced computational cells. The initial conditions for this flow are written in (3):

$$\bar{u}(t = 0) = \begin{bmatrix} \sin(x)\cos(y)\cos(z) \\ 0 \\ -\cos(x)\sin(y)\cos(z) \end{bmatrix} \quad (3)$$

Computation is executed for several values of Reynolds number. In figure 7 there is depicted decay of the total vorticity in time for Re 5000.

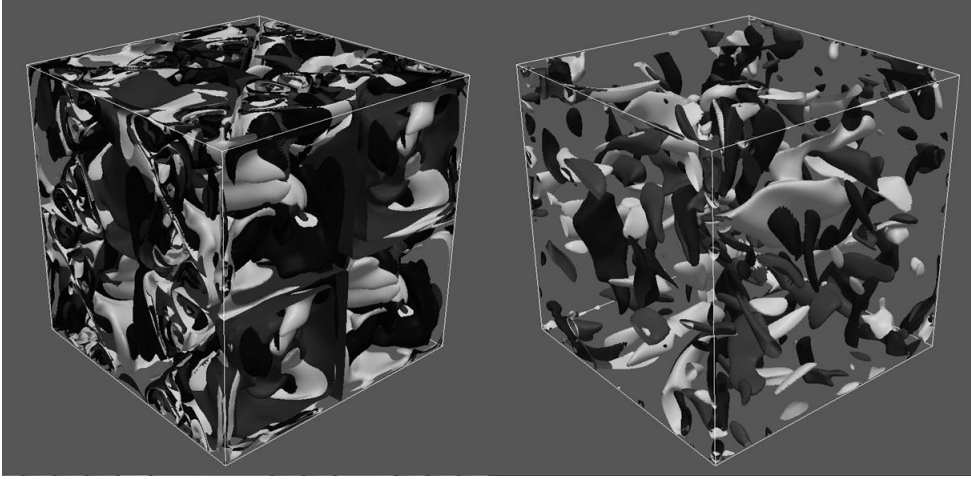


**Figure 7.** TGV, 3D view, components of vorticity, value 0.5. Decay of the vortices in time.  $t=0.75$  (left) and  $t=7.5$  (right) for Re 5000

The evolution in time of the kinetic energy  $E_K$ , where  $E_K = 1/2 \langle u^2 \rangle$  and  $\langle \rangle$  denotes mean (volumetric average), is demonstrated in Figure 8 as the dependence of several values of CFL for Re=1000 and in Figure 9 in the dependence on Reynolds number.

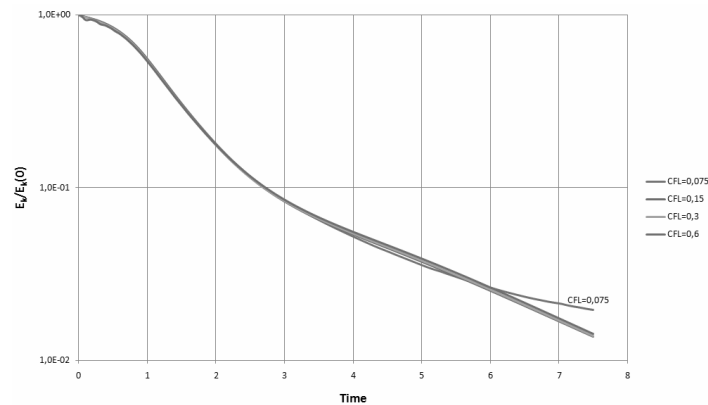


**Figure 8.** TGV, time evaluation of normalized kinetic energy in the dependence of CFL

The dependence of CFL on the computation of TGV shows for CFL in range 0.15 – 0.6 no significant differences. But for CFL 0.075 there are some changes.

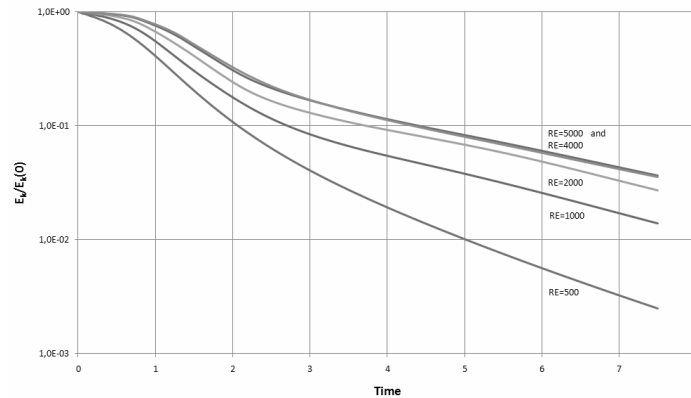


**Figure 9.** TGV, time evaluation of normalized kinetic energy in the dependence of Reynolds number

Variation of Reynolds numbers makes differences in the decreasing of normalized kinetic energy. The fastest decrease is for Re 500 and the slowest for Re 5000. The decrease of the Kinetic energy continues also after time  $t=7.5$ , in which the computation is stopped.

For Reynolds number equal to 2000 it is shown (figure 10) the count of kinetic energy for each control volume (CV) of computed area. It is clearly visible with time that the kinetic Energy goes for each CV to united value. After a long time it means, in the whole area it is the same value of kinetic energy. The isotropic turbulence is formed from the initial condition.

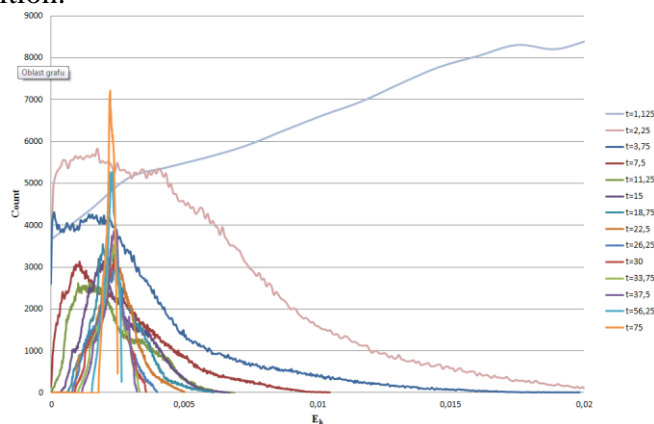


**Figure 10.** TGV, time evaluation of count of kinetic energy for each CV, Re 2000

## Conclusion

We employed a fifth-order WENO reconstruction of the convective terms of Navier–Stokes equations and the method ILES to compute 3D incompressible, turbulent flow motion. The three tested cases were modelled for different meshes, CFL's and Reynolds numbers. As turbulent flow examples, we computed lid-driven cavity flow for  $Re= 400-100\ 000$  with well developed vortexes. Next we computed flow past a cube for several Re numbers. For low value of Re flow became steady. For high Reynolds numbers the vortex street behind the obstacle were pronounced. Taylor-Green vortex case was solved for some values of Re numbers and stability conditions CFL's. With the

decreasing values of Reynolds numbers the faster decay of kinetic energy was observed. For the lowest value of CFL the solution was different against other used CFL's.

**Acknowledgments.** This research was supported by the Czech Ministry of Education, Youth and Sports under the framework of Research Plan MSM0021620860.

## References

- Brown, D. L., Cortez, R. and Minion, L. M., 2001: Accurate Projection Methods for the Incompressible Navier-Stokes Equations. *Journal of Computational Physics* 168, 464-499.
- Ferziger, J. H. and Peric, M., 1997: *Computational Methods for Fluid Dynamics*. Springer Verlag, Berlin.
- Don W.S., Gottlieb D., Shu Ch.W., Schilling O. and Jameson L., 2002, Numerical Convergence Study of Nearly-Incompressible, Inviscid Taylor-Green Vortex Flow
- Drikakis D., Fureby Ch., Grinstein F. F., Hahn M. and Youngs D., LES of Transition to Turbulence in the Taylor Green Vortex
- Ghia, U., Ghia, K. N. and Shin, C. T., 1982: High-Resolutions for Incompressible Flow Using the Navier-Stokes Equations and a Multigrid Method. *Journal of Computational Physics* 48, 387-411.
- Gottlieb, S. a Shu, C. W., 1998. Total Variation Diminishing Runge-Kutta Schemes. *Mathematics of Computation*, 67, 73-85
- Grinstein, F.F., Margolin, L. G. And Rider, W., 2007, *Implicit Large Eddy Simulation*, Cambridge University Press
- Harten, A., Enquist, B., Osher, S. a Chakravarthy, S.R., 1987. Uniformly High Order Accurate Essentially Non-Oscillatory Schemes, III. *Journal of Computational Physics* 71,231-303.
- Jirk, A., 2008: Thermally stratified atmospheric flow modelling. Diploma thesis. Dept of Meteorology and Env. Protect., MFF UK Prague (in Czech).
- Kim, J., Kim, D. and Choi, H., 2001: An immersed-Boundary Finite-Volume Method for Simulations of Flow in Complex Geometry. *Journal of Computational Physics* 171, 132-150.
- Liu, X. D., Osher, S. and Chan T., 1994: Weighted Essentially Non-Oscillatory Schemes. *Journal of Computational Physics* 115, 200-212.
- McDonough, J. M., 2003: *Lectures in Computational Fluid Dynamics of Incompressible Flow: Mathematics, Algorithms and Implementations*. Departments of Mechanical Engineering and Mathematics University of Kentucky.
- Shu, Ch.W. and Osher, S., 1988: Efficient Implementation of Essentially Non-Oscillatory Shock-Capturing Schemes, II. *Journal of Computational Physics* 83,32-78